



CERN-EP-2023-005  
23 January 2023

## Exploring the non-universality of charm hadronisation through the measurement of the fraction of jet longitudinal momentum carried by $\Lambda_c^+$ baryons in pp collisions

ALICE Collaboration

### Abstract

Recent measurements of charm-baryon production in hadronic collisions have questioned the universality of charm-quark fragmentation across different collision systems. In this work the fragmentation of charm quarks into charm baryons is probed, by presenting the first measurement of the longitudinal jet momentum fraction carried by  $\Lambda_c^+$  baryons,  $z_{\parallel}^{\text{ch}}$ , in hadronic collisions. The results are obtained in proton–proton (pp) collisions at  $\sqrt{s} = 13$  TeV at the LHC, with  $\Lambda_c^+$  baryons and track-based jets reconstructed in the transverse momentum intervals of  $3 \leq p_T^{\Lambda_c^+} < 15$  GeV/c and  $7 \leq p_T^{\text{jet ch}} < 15$  GeV/c, respectively. The  $z_{\parallel}^{\text{ch}}$  distribution is compared to a measurement of  $D^0$ -tagged charged jets in pp collisions as well as to PYTHIA 8 simulations. The data hints that the fragmentation of charm quarks into charm baryons is softer with respect to charm mesons, as predicted by hadronisation models which include colour correlations beyond leading-colour in the string formation.

arXiv:2301.13798v1 [nucl-ex] 31 Jan 2023

Heavy-flavour hadrons are produced in high-energy particle collisions through the fragmentation of heavy (charm and beauty) quarks, which typically originate in hard scattering processes in the early stages of the collisions. The most common theoretical approach to describe heavy-flavour production in hadronic collisions is based on the quantum chromodynamics (QCD) factorisation approach [1], and consists of a convolution of three independent terms: the parton distribution functions of the incoming hadrons, the cross sections of the partonic scattering producing the heavy quarks, and the fragmentation functions that parametrise the evolution of a heavy quark into given species of heavy-flavour hadrons. As the transition of quarks to hadrons cannot be described in perturbation theory, the fragmentation functions cannot be calculated and must be extracted from data.

Fragmentation functions of charm quarks to charm baryons and mesons have been constrained in  $e^+e^-$  and  $e^-p$  collisions [2–5], using a variety of different observables, such as the hadron momentum as a fraction of its maximum possible momentum, as dictated by the centre-of-mass energy of the collision. Another method to probe the fragmentation of quarks to hadrons is to parametrise the hadron momentum in relation to the momentum of jets, which are collimated bunches of hadrons giving experimental access to the properties of the scattered quark. Recently, the production of charm mesons in jets, probed via the fractional longitudinal momentum of the jet carried by the D meson, was measured in pp collisions at the Large Hadron Collider (LHC) [6–8] and appears consistent with Monte Carlo (MC) simulations tuned on  $e^+e^-$  data. These measurements support the assumption of fragmentation universality across collision systems in the charm-meson sector. This assumption underpins theoretical calculations describing the production of heavy-flavour hadrons in hadronic collisions, which make use of fragmentation functions tuned on  $e^+e^-$  and  $e^-p$  data.

Measurements of the production cross sections of baryons in pp collisions have questioned the hypothesis of fragmentation universality across collision systems [9]. In the charm sector, which provides a clean probe of hadronisation phenomena due to the large mass of the charm quark, recent measurements performed by the ALICE Collaboration [10–18] in pp collisions have shown that the ratio of the  $\Lambda_c^+$  (and other charm baryons) and  $D^0$  production cross sections measured at low  $p_T$  ( $\lesssim 12$  GeV/ $c$ ) is significantly larger than the value expected from MC simulations in which the charm fragmentation is tuned on  $e^+e^-$  and  $e^-p$  measurements, such as PYTHIA 8 [19] with the Monash tune [20] or HERWIG 7 [21]. A recent measurement of the  $\Lambda_c^+/D^0$  ratio in pp collisions, performed by the ALICE Collaboration in intervals of charged-particle multiplicity, also points to a substantial increase of the  $\Lambda_c^+/D^0$  ratio with increasing multiplicity, with respect to  $e^+e^-$  collisions, starting at very low multiplicities [14].

The study of charm-baryon production in jets can provide more differential insights into hadronisation mechanisms in pp collisions, compared to  $p_T$ -differential cross sections and yield ratios of heavy-flavour hadrons, allowing for a more accurate study of the dynamical properties of baryon production. In this letter, the first measurement of the longitudinal momentum fraction of the jet carried by  $\Lambda_c^+$  baryons,  $z_{\parallel}^{\text{ch}}$ , is presented. The measurement is performed in pp collisions at  $\sqrt{s} = 13$  TeV in the interval  $0.4 \leq z_{\parallel}^{\text{ch}} \leq 1.0$ . The  $z_{\parallel}^{\text{ch}}$  distribution, fully corrected to particle level, is presented for prompt (charm-quark initiated)  $\Lambda_c^+$ -tagged jets with  $7 \leq p_T^{\text{jet ch}} < 15$  GeV/ $c$  and  $3 \leq p_T^{\Lambda_c^+} < 15$  GeV/ $c$ . The results are then compared to PYTHIA 8 simulations [19, 22], including a version where mechanisms beyond the leading-colour approximation are considered in string formation processes during hadronisation [20], and to an analogous measurement of the  $z_{\parallel}^{\text{ch}}$  distribution of  $D^0$  mesons, performed by the ALICE Collaboration [6].

A full description of the ALICE setup and apparatus can be found in Refs. 23, 24. The main detectors used in this analysis are the Inner Tracking System (ITS), which is used for vertex reconstruction and tracking; the Time Projection Chamber (TPC), which is used for tracking and particle identification (PID); and the Time-Of-Flight (TOF) detector, which is used for PID. These detectors cover a pseudorapidity interval of  $|\eta| < 0.9$ . The analysis was performed on pp collisions at  $\sqrt{s} = 13$  TeV, collected using a minimum-bias (MB) trigger during the years 2016, 2017, and 2018. The trigger condition required

coincident signals in the two scintillator arrays of the V0 detector, with background events originating from beam–gas interactions removed offline using timing information from the V0. To mitigate against pile-up effects, events with multiple reconstructed primary vertices were rejected. To ensure uniform acceptance, only events with a primary-vertex position along the beam axis direction of  $|z_{\text{vtx}}| < 10$  cm around the nominal interaction point were accepted. After the selections described above, the data sample consisted of  $1.7 \times 10^9$  events, corresponding to an integrated luminosity of  $\mathcal{L}_{\text{int}} = 29 \text{ nb}^{-1}$  [25].

The  $\Lambda_c^+$  candidates and their charge conjugates were reconstructed via the hadronic  $\Lambda_c^+ \rightarrow pK_S^0 \rightarrow p\pi^+\pi^-$  decay channel with a total branching ratio of  $(1.10 \pm 0.06)\%$  [26], in the  $\Lambda_c^+$  transverse-momentum interval of  $3 \leq p_T^{\Lambda_c^+} < 15 \text{ GeV}/c$ . Only tracks with  $|\eta| < 0.8$  and  $p_T > 0.4 \text{ GeV}/c$ , which fulfilled the track quality selections described in Ref. 13, were considered for the  $\Lambda_c^+$  reconstruction. The  $\Lambda_c^+$  candidates themselves were reconstructed in the  $|y^{\Lambda_c^+}| < 0.8$  rapidity interval. The  $\Lambda_c^+$ -candidate selection was performed using a multivariate technique based on the Boosted Decision Tree (BDT) algorithm provided by the XGBoost package [27]. The features considered in the optimisation include the PID signal for the proton track, the invariant mass of the  $K_S^0$ -meson candidate, and topological variables that exploit the kinematic properties of the displaced  $K_S^0$ -meson decay vertex. The training was performed in intervals of  $\Lambda_c^+$ -candidate  $p_T$ , considering prompt signal candidates from PYTHIA 8 events with the Monash tune [19, 20], transported through a realistic description of the detector geometry and material budget using GEANT 3 [28]. Background candidates were extracted from the sidebands of the invariant-mass distributions in data. The probability thresholds of the BDT selections were tuned, using MC simulations, to maximise the statistical significance for the signal. Further details on the  $\Lambda_c^+$ -candidate reconstruction and machine learning procedure are provided in Ref. 14, where the same reconstruction and BDT model were employed.

For the events where at least one selected  $\Lambda_c^+$  candidate was identified, a jet-finding procedure was performed, using the FastJet package [29]. Prior to jet clustering, the  $\Lambda_c^+$ -candidate daughter tracks were replaced by the reconstructed  $\Lambda_c^+$ -candidate four-momentum vector. Track-based jet finding was carried out on charged tracks with  $|\eta| < 0.9$  and  $p_T > 0.15 \text{ GeV}/c$ , using the anti- $k_T$  algorithm [30], with a resolution parameter of  $R = 0.4$ . Tracks were combined using the  $E$ -scheme recombination [31], with the jet transverse momentum limited to the interval of  $5 \leq p_T^{\text{jet ch}} < 35 \text{ GeV}/c$ . The full jet cone was required to be within the ALICE central barrel acceptance, limiting the jet axis to the interval  $|\eta_{\text{jet}}| < 0.5$ . Only jets tagged via the presence of a reconstructed  $\Lambda_c^+$  candidate amongst their constituents were considered for the analysis. For events where more than one  $\Lambda_c^+$  candidate was found, the jet finding and tagging pass was performed independently for each candidate, with only the daughters of that particular candidate replaced by the corresponding  $\Lambda_c^+$  four-vector each time. In mechanisms of hadronisation that include colour correlations beyond the leading-colour approximation [20], which have been shown to be relevant in hadronic collisions at LHC energies [9], hadrons can be formed in processes that combine quarks from the parton shower with those from the underlying event [32]. As such, the underlying event is not well defined with respect to the measured hadron distributions. Therefore no underlying event correction is implemented in this work.

The fragmentation of charm quarks to  $\Lambda_c^+$  baryons is probed by measuring the fraction of the jet momentum carried by the  $\Lambda_c^+$  along the direction of the jet axis,  $z_{\parallel}^{\text{ch}}$ . This is calculated for each jet using

$$z_{\parallel}^{\text{ch}} = \frac{\mathbf{p}_{\text{jet}} \cdot \mathbf{p}_{\Lambda_c^+}}{\mathbf{p}_{\text{jet}} \cdot \mathbf{p}_{\text{jet}}}, \quad (1)$$

where  $\mathbf{p}_{\text{jet}}$  and  $\mathbf{p}_{\Lambda_c^+}$  are the jet and  $\Lambda_c^+$  three-momentum vectors, respectively.

The  $z_{\parallel}^{\text{ch}}$  distributions of true  $\Lambda_c^+$ -tagged jets were extracted in intervals of  $\Lambda_c^+$   $p_T$  and  $p_T^{\text{jet ch}}$  using a sideband subtraction procedure. To enact this subtraction, the invariant-mass ( $m_{\text{inv}}$ ) distributions of  $\Lambda_c^+$  candidates, obtained for each  $\Lambda_c^+$   $p_T$  and  $p_T^{\text{jet ch}}$  interval, were fitted with a function comprising a Gaussian for the signal

and an exponential for the background. The fit parameters were then used to define signal (containing the majority of true signal candidates) and sideband (entirely composed of background candidates) regions, defined by  $|m_{\text{inv}} - \mu_{\text{fit}}| < 2\sigma_{\text{fit}}$  and  $4\sigma_{\text{fit}} < |m_{\text{inv}} - \mu_{\text{fit}}| < 9\sigma_{\text{fit}}$ , respectively, where  $\mu_{\text{fit}}$  and  $\sigma_{\text{fit}}$  represent the mean and sigma of the fitted Gaussian distributions. The  $z_{\parallel}^{\text{ch}}(p_{\text{T}}^{\Lambda_c^+}, p_{\text{T}}^{\text{jet ch}})$  distributions were extracted in the signal and sideband regions, with the sideband distribution scaled by the ratio of the background function integrals in the signal and sideband regions. The sideband distribution was then subtracted from the signal one, with the resulting distribution scaled to account for the fact that the  $2\sigma_{\text{fit}}$  width of the signal region only encompasses approximately 95% of the total signal, to obtain the sideband subtracted  $z_{\parallel}^{\text{ch}}$  yield in each  $p_{\text{T}}^{\Lambda_c^+}$  and  $p_{\text{T}}^{\text{jet ch}}$  interval.

To account for the reconstruction and selection efficiency of the  $\Lambda_c^+$ -tagged jet signal, the sideband subtracted  $z_{\parallel}^{\text{ch}}$  distributions in each  $p_{\text{T}}^{\Lambda_c^+}$  and  $p_{\text{T}}^{\text{jet ch}}$  interval,  $N(z_{\parallel}^{\text{ch}}, p_{\text{T}}^{\Lambda_c^+}, p_{\text{T}}^{\text{jet ch}})$ , were scaled by the reconstruction efficiency of prompt  $\Lambda_c^+$ -tagged jets,  $\epsilon_{\text{prompt}}$ , and summed over the entire  $p_{\text{T}}^{\Lambda_c^+}$  interval to obtain the efficiency-corrected  $z_{\parallel}^{\text{ch}}$  yield of  $\Lambda_c^+$ -tagged jets,  $N^{\text{corr}}(z_{\parallel}^{\text{ch}}, p_{\text{T}}^{\text{jet ch}})$ , given by

$$N^{\text{corr}}(z_{\parallel}^{\text{ch}}, p_{\text{T}}^{\text{jet ch}}) = \sum_{p_{\text{T}}^{\Lambda_c^+}} \frac{N(z_{\parallel}^{\text{ch}}, p_{\text{T}}^{\Lambda_c^+}, p_{\text{T}}^{\text{jet ch}})}{\epsilon_{\text{prompt}}(p_{\text{T}}^{\Lambda_c^+})}. \quad (2)$$

The  $\epsilon_{\text{prompt}}(p_{\text{T}}^{\Lambda_c^+})$  efficiency is strongly dependent on  $p_{\text{T}}^{\Lambda_c^+}$ , ranging from about 20% at  $3 < p_{\text{T}}^{\Lambda_c^+} < 4$  GeV/ $c$  to 40% at  $12 < p_{\text{T}}^{\Lambda_c^+} < 24$  GeV/ $c$ , and was calculated using PYTHIA 8 simulations with the Monash tune containing prompt  $\Lambda_c^+$ -tagged jets, transported through the detector using GEANT 3. This efficiency does not exhibit a  $p_{\text{T}}^{\text{jet ch}}$  dependence.

In order to isolate the  $N^{\text{corr}}(z_{\parallel}^{\text{ch}}, p_{\text{T}}^{\text{jet ch}})$  distribution of prompt  $\Lambda_c^+$ -tagged jets, a feed-down subtraction was employed to remove the non-prompt (beauty-quark initiated) contribution. The non-prompt cross section was obtained from particle level POWHEG [33] + PYTHIA 6 [34] + EvtGen [35] simulations, as a function of  $p_{\text{T}}^{\text{jet ch}}$ ,  $p_{\text{T}}^{\Lambda_c^+}$  and  $z_{\parallel}^{\text{ch}}$ , and was scaled according to the integrated luminosity of the analysed data sample and the branching ratio of the  $\Lambda_c^+ \rightarrow pK_S^0 \rightarrow p\pi^+\pi^-$  decay channel. The resulting particle-level yield was multiplied by the ratio of the non-prompt to prompt  $\Lambda_c^+$ -tagged jet reconstruction and selection efficiency in intervals of  $p_{\text{T}}^{\Lambda_c^+}$  and integrated over the  $p_{\text{T}}^{\Lambda_c^+}$  range. The simulated non-prompt results were then folded to reconstructed level, using a four-dimensional response matrix generated using non-prompt  $\Lambda_c^+$ -tagged jets in PYTHIA 8 with the Monash tune, transported through a simulation of the ALICE detector using GEANT 3. The response matrix was constructed as a function of  $p_{\text{T}}^{\text{jet ch}}$  and  $z_{\parallel}^{\text{ch}}$  at generator and reconstruction levels. The folded results were then subtracted from the measured  $N^{\text{corr}}(z_{\parallel}^{\text{ch}}, p_{\text{T}}^{\text{jet ch}})$  distribution in data, removing the non-prompt contribution. The estimated fraction of  $\Lambda_c^+$ -tagged jets coming from b-quark fragmentation is found to be about 5%, with no significant  $z_{\parallel}^{\text{ch}}$  dependence.

A two-dimensional Bayesian unfolding procedure [36] was performed to correct for detector effects and obtain the  $z_{\parallel}^{\text{ch}}$  distribution for prompt  $\Lambda_c^+$ -tagged jets at particle level. A four-dimensional response matrix as a function of  $p_{\text{T}}^{\text{jet ch}}$  and  $z_{\parallel}^{\text{ch}}$ , at generator and reconstruction levels, was populated with prompt  $\Lambda_c^+$ -tagged jets, obtained with PYTHIA 8 simulations with the Monash tune, passed through a simulation of the ALICE detector using GEANT 3. The measured data and response matrix were provided in the intervals of  $5 \leq p_{\text{T}}^{\text{jet ch}} < 35$  GeV/ $c$  and  $0.4 \leq z_{\parallel}^{\text{ch}} \leq 1.0$ , with the final unfolded results reported in the intervals  $7 \leq p_{\text{T}}^{\text{jet ch}} < 15$  GeV/ $c$  and  $0.4 \leq z_{\parallel}^{\text{ch}} \leq 1.0$ . Corrections accounting for migrating entries in and out of the response matrix ranges, as modelled by the same MC simulation, were also applied. The corrected  $z_{\parallel}^{\text{ch}}$  distribution is normalised to the total number of  $\Lambda_c^+$ -tagged jets in the reported  $z_{\parallel}^{\text{ch}}$  and  $p_{\text{T}}^{\text{jet ch}}$  interval.

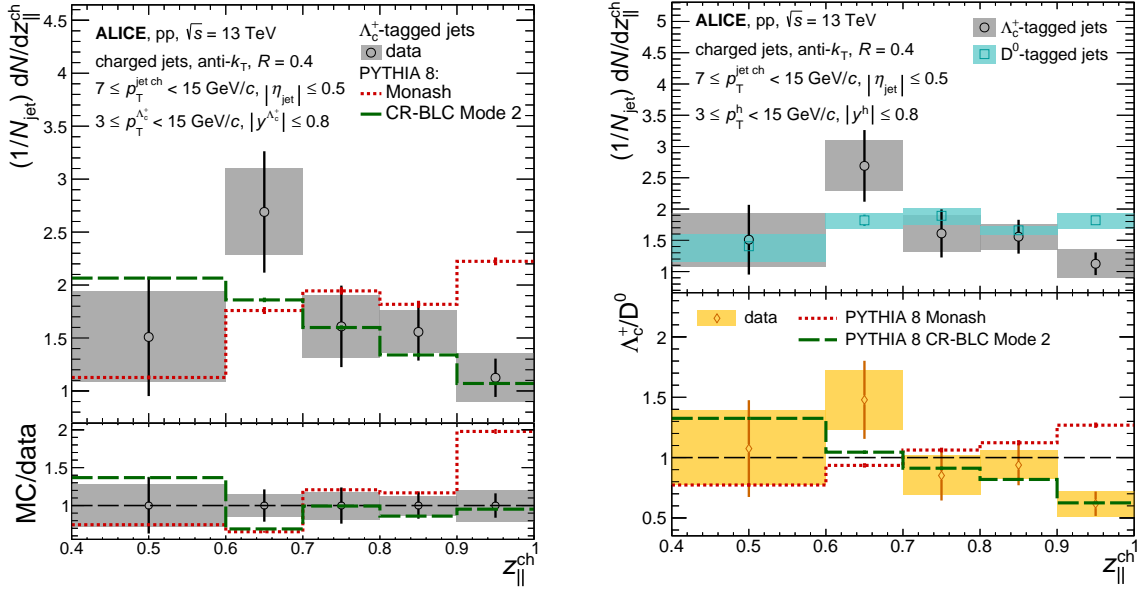


**Figure 1:** (Left) Fully corrected  $z_{||}^{\text{ch}}$  distribution of  $\Lambda_c^+$ -tagged track-based jets (black open circles) measured in the  $7 \leq p_T^{\text{jet ch}} < 15$  GeV/c and  $3 \leq p_T^{\Lambda_c^+} < 15$  GeV/c intervals in pp collisions at  $\sqrt{s} = 13$  TeV, compared with predictions from different PYTHIA 8 tunes [19, 20, 22] (red-dotted and green-dashed lines). The ratios of the MC simulations to the data are shown in the bottom panel. (Right) Comparison of the measured  $z_{||}^{\text{ch}}$  distribution of  $\Lambda_c^+$ -tagged jets and the previously measured  $z_{||}^{\text{ch}}$  distribution of  $D^0$ -tagged jets [6], obtained in the same kinematic interval. The ratio of the  $z_{||}^{\text{ch}}$  distribution of  $\Lambda_c^+$ -tagged and  $D^0$ -tagged jets is shown in the bottom panel for both the data and the different PYTHIA tunes.

The systematic uncertainties affecting the measurement were evaluated, in each  $z_{||}^{\text{ch}}$  interval, by modifying the strategy adopted at various steps of the analysis procedure and assessing the impact on the unfolded  $z_{||}^{\text{ch}}$  distribution. The total systematic uncertainty includes contributions from multiple sources. The first considered source is the sideband subtraction procedure (ranging from 3.7% to 7.6% depending on the  $z_{||}^{\text{ch}}$  interval), whose contribution was estimated by varying the invariant-mass fit parameters as well as the invariant-mass intervals of the signal and sideband regions. The contribution from the BDT selection of  $\Lambda_c^+$  candidates (from 7.3% to 19%) was estimated by varying the BDT probability thresholds to induce a 25% variation in the  $\Lambda_c^+$ -tagged jet reconstruction and selection efficiency. The uncertainty from the jet energy resolution (from 4.5% to 19%) was estimated by recalculating the response matrix used for unfolding with a 4% reduced tracking efficiency. The reduction in the tracking efficiency was evaluated by varying the track-selection criteria and propagating the ITS–TPC track-matching efficiency uncertainty. The uncertainty on the feed-down subtraction ( $< 2\%$ ) was estimated by varying the choice of POWHEG parameters considered to generate the feed-down cross section, including the factorisation and renormalisation scales, as well as the mass of the beauty quark, which were varied according to theoretical prescriptions [37]. Finally the contribution from the unfolding procedure (from 1.1% to 2.7%) was estimated by altering the choice of prior, regularisation parameter, and ranges of the response matrix. For each of the aforementioned categories, several variations were made and the root-mean-square of the resulting distributions was considered. The exceptions are related to the contribution associated to the choice of parameters of the POWHEG calculations, where only the largest deviation from the central result, in each direction, was considered, as well as the uncertainty on the jet energy resolution where the variation with respect to the central result was taken as the uncertainty. All uncertainties (other than from the feed-down subtraction) were then symmetrised. The uncertainties were combined in quadrature to obtain the total systematic uncertainty on the measurement, which ranges from 13% to 28%.

The fully corrected  $z_{||}^{\text{ch}}$  distribution of prompt  $\Lambda_c^+$ -tagged track-based jets in the intervals of  $7 \leq p_T^{\text{jet ch}} < 15$  GeV/ $c$  and  $3 \leq p_T^{\Lambda_c^+} < 15$  GeV/ $c$  is presented in the left-hand panel of Fig. 1 and compared to PYTHIA 8 simulations with two different tunes. In PYTHIA 8 the Lund string model of fragmentation is employed, where endpoints are confined by linear potentials encoded in strings. For the case of heavy quarks, the Lund fragmentation function is modified to account for the slower propagation of the massive endpoints compared to their massless counterparts. The Monash tune (red-dotted line) [19], in which the charm fragmentation is tuned on  $e^+e^-$  measurements, predicts a harder fragmentation than the measurement. An evaluation of the  $\chi^2/\text{ndf}$  between the measured data points and the model was performed, combining the statistical and systematic uncertainties on the data in quadrature and assuming the uncertainties are uncorrelated across the  $z_{||}^{\text{ch}}$  intervals. This exercise determines that there is a 0.4% probability that the model describes the data. A better agreement is achieved by the PYTHIA 8 with the CR-BLC Mode 2 tune, that includes colour reconnection mechanisms beyond the leading-colour approximation [22] (green-dashed line). In this model, the minimisation of the string potential is implemented considering the SU(3) multiplet structure of QCD in a more realistic way than in the leading-colour approximation, allowing for the formation of ‘‘baryonic’’ configurations where for example two colours can combine coherently to form an anti-colour. The same  $\chi^2/\text{ndf}$  approach results in a 78% probability that the model describes the data. The simulation with PYTHIA 8 with the CR-BLC Mode 2 tune also provides a much more accurate description of the  $\Lambda_c^+/D^0$  cross section ratio, previously measured in pp collisions at the LHC [10–14, 38].

In the right-hand panel of Fig. 1, a comparison of the  $z_{||}^{\text{ch}}$  distribution of  $\Lambda_c^+$ -tagged jets and the  $z_{||}^{\text{ch}}$  distribution previously measured for  $D^0$ -tagged jets [6] is presented. The latter is consistent with PYTHIA 8 simulations using both the Monash and CR-BLC Mode 2 tunes. The ratio of the two distributions is also presented in the bottom panel. The uncertainty from the jet energy resolution was considered to be correlated between the  $\Lambda_c^+$ -tagged jet and  $D^0$ -tagged jet measurements and was evaluated directly on the ratio of the distributions. The remaining uncertainties were considered uncorrelated when taking the ratio and were then combined in quadrature with the uncertainty of the jet energy resolution. The uncertainties were considered uncorrelated across the  $z_{||}^{\text{ch}}$  intervals. The same  $\chi^2/\text{ndf}$  exercise described above determines that there is a 12% probability that the measured ratio is described by a flat distribution at unity, hinting at a softer fragmentation of charm quarks into charm baryons than charm mesons. The ratio is better described by the PYTHIA 8 simulations with the CR-BLC Mode 2 compared to the ones with the Monash tune, with the former describing the data with 88% probability compared to a 0.03% probability for the latter.

In summary the first measurement in hadronic collisions of the longitudinal momentum fraction of the jet carried by  $\Lambda_c^+$  baryons was presented for pp collisions at  $\sqrt{s} = 13$  TeV. The result is fully corrected to particle level and obtained in the jet and  $\Lambda_c^+$  transverse-momentum intervals of  $7 \leq p_T^{\text{jet ch}} < 15$  GeV/ $c$  and  $3 \leq p_T^{\Lambda_c^+} < 15$  GeV/ $c$ , respectively. The measurement presented in this Letter hints that charm quarks have a softer fragmentation into  $\Lambda_c^+$  baryons compared to  $D^0$  mesons, in the measured kinematic interval. One possible explanation is that charm-baryon production is favoured in the presence of higher particle multiplicity originating from both the jet fragmentation and the underlying event, which could be tested with future measurements of the in-jet multiplicity of  $\Lambda_c^+$ -tagged jets. The fragmentation of charm quarks into  $\Lambda_c^+$  baryons in hadronic collisions exhibits tension with simulations tuned on  $e^+e^-$  data that employ a leading-colour formalism of hadronisation, such as in the Monash tune of PYTHIA 8. This occurs despite their successful description of the fragmentation of charm quarks into  $D^0$  mesons. However, the inclusion of mechanisms sensitive to the surrounding partonic density that feature colour reconnection beyond the leading-colour approximation results in a better agreement with data. This result also partially explains the  $p_T$  shape of the prompt  $\Lambda_c^+/D^0$  cross section ratio [10–14, 38], which shows a peak at low  $p_T$  ( $\approx 3$  GeV/ $c$ ) and is also described within uncertainties by PYTHIA 8 with the CR-BLC Mode 2 tune. The  $p_T$  trend of this ratio is driven by the fact that the  $\Lambda_c^+$  baryons produced from the fragmenting charm quark carry a significantly lower fraction of the charm-quark transverse momentum than the  $D^0$  mesons

produced in a similar way.

## References

- [1] J. C. Collins, D. E. Soper, and G. F. Sterman, “Factorization of Hard Processes in QCD”, *Adv. Ser. Direct. High Energy Phys.* **5** (1989) 1–91, arXiv:hep-ph/0409313.
- [2] **ALEPH** Collaboration, R. Barate *et al.*, “Study of charm production in Z decays”, *Eur. Phys. J. C* **16** (2000) 597–611, arXiv:hep-ex/9909032.
- [3] **Belle** Collaboration, R. Seuster *et al.*, “Charm hadrons from fragmentation and B decays in  $e^+e^-$  annihilation at  $\sqrt{s} = 10.6$  GeV”, *Phys. Rev. D* **73** (2006) 032002, arXiv:hep-ex/0506068.
- [4] **ZEUS** Collaboration, S. Chekanov *et al.*, “Measurement of the charm fragmentation function in  $D^*$  photoproduction at HERA”, *JHEP* **04** (2009) 082, arXiv:0901.1210 [hep-ex].
- [5] **Belle** Collaboration, M. Niiyama *et al.*, “Production cross sections of hyperons and charmed baryons from  $e^+e^-$  annihilation near  $\sqrt{s} = 10.52$  GeV”, *Phys. Rev. D* **97** (2018) 072005, arXiv:1706.06791 [hep-ex].
- [6] **ALICE** Collaboration, S. Acharya *et al.*, “Measurement of the production of charm jets tagged with  $D^0$  mesons in pp collisions at  $\sqrt{s} = 5.02$  and 13 TeV”, arXiv:2204.10167 [nucl-ex].
- [7] **ALICE** Collaboration, S. Acharya *et al.*, “Measurement of the production of charm jets tagged with  $D^0$  mesons in pp collisions at  $\sqrt{s} = 7$  TeV”, *JHEP* **08** (2019) 133, arXiv:1905.02510 [nucl-ex].
- [8] **ATLAS** Collaboration, G. Aad *et al.*, “Measurement of  $D^{*\pm}$  meson production in jets from pp collisions at  $\sqrt{s} = 7$  TeV with the ATLAS detector”, *Phys. Rev. D* **85** (2012) 052005, arXiv:1112.4432 [hep-ex].
- [9] **ALICE** Collaboration, J. Adam *et al.*, “Enhanced production of multi-strange hadrons in high-multiplicity proton-proton collisions”, *Nature Phys.* **13** (2017) 535–539, arXiv:1606.07424 [nucl-ex].
- [10] **ALICE** Collaboration, S. Acharya *et al.*, “ $\Lambda_c^+$  production in pp collisions at  $\sqrt{s} = 7$  TeV and in p–Pb collisions at  $\sqrt{s_{NN}} = 5.02$  TeV”, *JHEP* **04** (2018) 108, arXiv:1712.09581 [nucl-ex].
- [11] **ALICE** Collaboration, S. Acharya *et al.*, “ $\Lambda_c^+$  Production and Baryon-to-Meson Ratios in pp and p–Pb Collisions at  $\sqrt{s_{NN}} = 5.02$  TeV at the LHC”, *Phys. Rev. Lett.* **127** (2021) 202301, arXiv:2011.06078 [nucl-ex].
- [12] **ALICE** Collaboration, S. Acharya *et al.*, “Measurement of Prompt  $D^0$ ,  $\Lambda_c^+$ , and  $\Sigma_c^{0,++}(2455)$  Production in Proton–Proton Collisions at  $\sqrt{s} = 13$  TeV”, *Phys. Rev. Lett.* **128** (2022) 012001, arXiv:2106.08278 [hep-ex].
- [13] **ALICE** Collaboration, S. Acharya *et al.*, “ $\Lambda_c^+$  production in pp and in p–Pb collisions at  $\sqrt{s_{NN}} = 5.02$  TeV”, *Phys. Rev. C* **104** (2021) 054905, arXiv:2011.06079 [nucl-ex].
- [14] **ALICE** Collaboration, S. Acharya *et al.*, “Observation of a multiplicity dependence in the  $p_T$ -differential charm baryon-to-meson ratios in proton–proton collisions at  $\sqrt{s} = 13$  TeV”, *Phys. Lett. B* **829** (2022) 137065, arXiv:2111.11948 [nucl-ex].
- [15] **ALICE** Collaboration, S. Acharya *et al.*, “Charm-quark fragmentation fractions and production cross section at midrapidity in pp collisions at the LHC”, *Phys. Rev. D* **105** (2022) L011103, arXiv:2105.06335 [nucl-ex].

- [16] **ALICE** Collaboration, “First measurement of  $\Omega_c^0$  production in pp collisions at  $\sqrt{s} = 13$  TeV”, arXiv:2205.13993 [nucl-ex].
- [17] **ALICE** Collaboration, S. Acharya *et al.*, “First measurement of  $\Xi_c^0$  production in pp collisions at  $\sqrt{s} = 7$  TeV”, *Phys. Lett. B* **781** (2018) 8–19, arXiv:1712.04242 [hep-ex].
- [18] **ALICE** Collaboration, S. Acharya *et al.*, “Measurement of the Cross Sections of  $\Xi_c^0$  and  $\Xi_c^+$  Baryons and of the Branching-Fraction Ratio  $\text{BR}(\Xi_c^0 \rightarrow \Xi^- e^+ \nu_e)/\text{BR}(\Xi_c^0 \rightarrow \Xi^- \pi^+)$  in pp collisions at 13 TeV”, *Phys. Rev. Lett.* **127** (2021) 272001, arXiv:2105.05187 [nucl-ex].
- [19] P. Skands, S. Carrazza, and J. Rojo, “Tuning PYTHIA 8.1: the Monash 2013 Tune”, *Eur. Phys. J. C* **74** (2014) 3024, arXiv:1404.5630 [hep-ph].
- [20] T. Sjöstrand *et al.*, “An introduction to PYTHIA 8.2”, *Comput. Phys. Commun.* **191** (2015) 159–177, arXiv:1410.3012 [hep-ph].
- [21] M. Bahr *et al.*, “Herwig++ Physics and Manual”, *Eur. Phys. J. C* **58** (2008) 639–707, arXiv:0803.0883 [hep-ph].
- [22] J. R. Christiansen and P. Z. Skands, “String Formation Beyond Leading Colour”, *JHEP* **08** (2015) 003, arXiv:1505.01681 [hep-ph].
- [23] **ALICE** Collaboration, K. Aamodt *et al.*, “The ALICE experiment at the CERN LHC”, *JINST* **3** (2008) S08002.
- [24] **ALICE** Collaboration, B. B. Abelev *et al.*, “Performance of the ALICE Experiment at the CERN LHC”, *Int. J. Mod. Phys. A* **29** (2014) 1430044, arXiv:1402.4476 [nucl-ex].
- [25] **ALICE** Collaboration, S. Acharya *et al.*, “ALICE 2016-2017-2018 luminosity determination for pp collisions at  $\sqrt{s} = 13$  TeV”, <https://cds.cern.ch/record/2776672>.
- [26] **Particle Data Group** Collaboration, P. Zyla *et al.*, “Review of Particle Physics”, *PTEP* **2020** (2020) 083C01.
- [27] T. Chen and C. Guestrin, “XGBoost: A scalable tree boosting system”, in *Proceedings of the 22nd ACM SIGKDD International Conference on Knowledge Discovery and Data Mining, KDD ’16*, pp. 785–794. ACM, 2016. arXiv:1603.02754 [cs.LG].
- [28] R. Brun, F. Bruyant, M. Maire, A. C. McPherson, and P. Zancarini, *GEANT 3 : user’s guide Geant 3.10, Geant 3.11; rev. version*. CERN, Geneva, 1987. <https://cds.cern.ch/record/1119728>.
- [29] M. Cacciari, G. P. Salam, and G. Soyez, “FastJet user manual”, *Eur. Phys. J. C* **72** (2012) 1896, arXiv:1111.6097 [hep-ph].
- [30] M. Cacciari, G. P. Salam, and G. Soyez, “The anti- $k_t$  jet clustering algorithm”, *JHEP* **04** (2008) 063, arXiv:0802.1189 [hep-ph].
- [31] M. Cacciari, G. P. Salam, and G. Soyez, “The Catchment Area of Jets”, *JHEP* **04** (2008) 005, arXiv:0802.1188 [hep-ph].
- [32] K. C. Han, R. J. Fries, and C. M. Ko, “Jet Fragmentation via Recombination of Parton Showers”, *Phys. Rev. C* **93** (2016) 045207, arXiv:1601.00708 [nucl-th].
- [33] S. Alioli, P. Nason, C. Oleari, and E. Re, “A general framework for implementing NLO calculations in shower Monte Carlo programs: the POWHEG BOX”, *JHEP* **06** (2010) 043, arXiv:1002.2581 [hep-ph].



- [34] T. Sjöstrand, S. Mrenna, and P. Z. Skands, “PYTHIA 6.4 Physics and Manual”, *JHEP* **05** (2006) 026, arXiv:hep-ph/0603175.
- [35] D. J. Lange, “The EvtGen particle decay simulation package”, *Nuclear Instruments and Methods in Physics Research Section A: Accelerators, Spectrometers, Detectors and Associated Equipment* **462** (2001) 152–155.
- [36] G. D’Agostini, “A multidimensional unfolding method based on Bayes’ theorem”, *Nucl. Instrum. Meth. A* **362** (1995) 487–498.
- [37] M. Cacciari, P. Nason, and R. Vogt, “QCD predictions for charm and bottom production at RHIC”, *Phys. Rev. Lett.* **95** (2005) 122001, arXiv:hep-ph/0502203.
- [38] CMS Collaboration, A. M. Sirunyan *et al.*, “Production of  $\Lambda_c^+$  baryons in proton-proton and lead-lead collisions at  $\sqrt{s_{NN}} = 5.02$  TeV”, *Phys. Lett. B* **803** (2020) 135328, arXiv:1906.03322 [hep-ex].